NWP SAF

Satellite Application Facility
for Numerical Weather Prediction

Document NWPSAF-KN-TR-003

Version 1.2

22-10-2014

The orientation of SeaWinds wind vector cells

Jur Vogelzang and Anton Verhoef

KNMI, De Bilt, The Netherlands

The EUMETSAT Network of Satellite Application Facilities

NWP SAF
Numerical Weather Prediction

Met Office

ECMWF

Royal Netherlands Meteorological Institute
Ministry of Infrastructure and the Environment

METEO FRANCE
Toujours un temps d'avance

The orientation of SeaWinds wind vector cells

Jur Vogelzang and Anton Verhoef

KNMI, De Bilt, The Netherlands

This documentation was developed within the context of the EUMETSAT Satellite Application Facility on Numerical Weather Prediction (NWP SAF), under the Cooperation Agreement dated 29 June, 2011, between EUMETSAT and the Met Office, UK, by one or more partners within the NWP SAF. The partners in the NWP SAF are the Met Office, ECMWF, KNMI and Météo France.

Change record				
Version	Date	Author	Approved	Remarks
1.0	Sept 2006	Jur Vogelzang	--	First draft
1.1	Dec 2006	Jur Vogelzang	Ad Stoffelen	Comments by Ad Stoffelen and Marcos Portabella
1.2	Oct 2014	Jur Vogelzang	Ad Stoffelen	Corrected some errors in section 2.3 and added chapter 6.

Contents

1 Introduction

1.1 Aims and scope

The orientation of the SeaWinds Wind Vector Cells (WVC's) is needed in 2DVAR and in program ASAC for calculating autocorrelations. In both cases the wind field is to be separated into components perpendicular and tangential to the satellite moving direction, P and T respectively. Note that P is also referred to as the transversal wind component and T as the longitudinal component. At the centre of the swath, the orientation equals the heading of the satellite.

The orientation of a WVC, denoted as α, is defined as the angle that the ground projection of that WVC in the direction of increasing row number makes with the local meridian, measured counterclockwise from the north. It is a function of the geographical latitude ϕ and WVC number. With this definition the wind components P and T are defined as

$$\begin{aligned} P &= u\cos\alpha + v\sin\alpha \\ T &= -u\sin\alpha + v\cos\alpha \end{aligned} , \tag{1.1}$$

with u and v the zonal (west-to-east) and meridional (south-to-north) wind components, respectively.

Presently, the software for 2DVAR and statistical processing contains different algorithms to calculate the orientation of a WVC. In general, the orientation of a WVC will depend on the geographical latitude and its WVC number. It is the aim of this study to intercompare these methods and alternatives for finding the optimal method in terms of accuracy, stability, and computational efficiency.

A suitable method should fulfill the following requirements:

- It should be applicable for each WVC in a row;
- It should be precise, stable, and accurate

1.2 Outline

Four methods for calculating the WVC orientation from information available from the BUFR input files are introduced in chapter 2. For each method a derivation is given of the orientation and its error. The four methods include current methods used in 2DVAR and statistical analysis.

The four methods are compared with each other in chapter 3. Only one method is found to fulfill all requirements. This method is based on a great spherical triangle formed by two WVC's and the North Pole. Only the geographic positions of the two WVC's are needed. Its accuracy is 1° or better.

Chapter 4 contains a short note on the heading of the satellite. It can be found by averaging the orientation of the two central WVC's, but there is also an alternative method based on spherical triangles that is complementary in precision. This method is presented and some results are given.

Chapter 5 describes how the results are incorporated in 2DVAR and what effect the new algorithm for finding the WVC orientations has on the wind field.

Chapter 6 deals with how the algorithm works for other platforms, in particular for RapidSCAT on board the International Space Station (ISS).

Chapter 7 ends with the conclusions. The most important conclusion is that the methods currently implemented in 2DVAR are far from optimal and badly need modification.

2 Methods

2.1 Introduction and overview

Figure 2.1 shows an overview of the measurement geometry and the orientations of the Wind Vector Cells (WVC's). The orbit of QuikSCAT, at 803 km height, is in yellow. The ground projection of the orbit is in grey. Perpendicular to that, as a red line, is a row of WVC's. The orientation of the WVC's is indicated by the red arrows. It is perpendicular to the row, but near the ends of the swath the WVC orientation differs from the direction of the orbit ground projection.

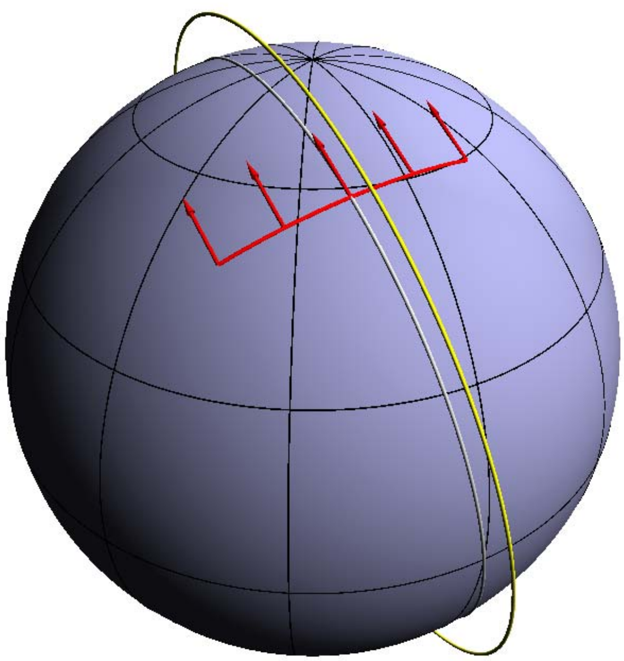

Figure 2.1 SeaWinds measurement geometry and WVC orientation.

The SeaWinds BUFR messages contain no information on the orientation of the WVC's. The only directional information similar to this is the satellite's heading, given as the second number in each subset of the BUFR messages. For an odd number of WVC's on a row (100 km resolution), the satellite heading equals the orientation of the central WVC. For an even number of WVC's (resolution 50 km or 25 km), the satellite heading lies between the orientations of the two central WVC's.

The heading is given with a precision of 1°, which is rather coarse. More important, it is only given for rows that contain at least one wind measurement. It has no global coverage, as can be seen from figure 2.2, which rules out application in 2DVAR. Figure 2.2 was obtained using the first three BUFR files of December 1, 2002. The three files span a little more than one orbit. Notably at higher and lower latitudes no heading is available.

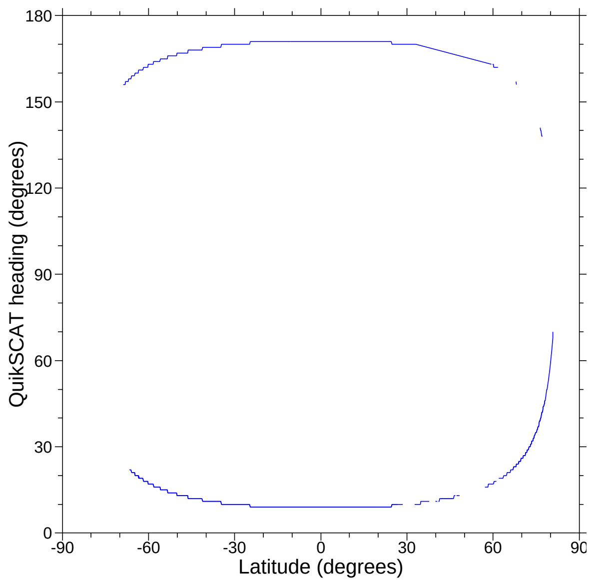

Figure 2.2 Satellite heading in the BUFR message versus latitude for the first three BUFR messages of December 1, 2002, covering a bit more than one orbit.

There are four methods (at least) to calculate the heading of a SeaWinds WVC from the data available in the BUFR messages:

1: Planimetric calculation of the orientation of the line joining two WVC's on the same row. This method is used in program `ASAC` to calculate the autocorrelations, with the WVC's far apart (WVC 10 and 67). The variation of the orientation with WVC number is neglected.

2: Spherical trigoniometric calculation from the positions of two WVC's on a row using a great spherical triangle formed by two WVC's and the North Pole. This method was used in the old `SpatCor` program (the precursor of `ASAC`) for calculating autocorrelations. The program used adjacent WVC's for calculating the orientation.

3: Spherical trigoniometric calculation from the positions of two WVC's and their distance on a row using a great spherical triangle formed by two WVC's and the North Pole. This method is a variant of method 2: it employs the same great triangle but different information.

4: Stereometric calculation from the positions of two WVC's. This method is presently used in 2DVAR. The orientation of a vector connecting two adjacent WVC's is used as orientation of the rightmost WVC.

The position of the WVC's is given for each row, at least for WVC numbers 2 to 75 (at 25 km resolution), except for a semicircle at the start and end of each BUFR input file. However, there is generally plenty of overlap between the BUFR files to fill the gaps between them. The geographical latitude and longitude, ϕ and λ, are given up to 0.01° precision, so the errors are $\delta\phi = \delta\lambda = 0.005^{\circ}$. Assuming the radius of the Earth equal to 6378 km (this is the equatorial radius), the error in each of the geographical coordinates amounts to an error in position of 0.56 km at most.

The orientations may contain two types of errors:

- errors caused by propagation of the errors in the WVC coordinates, and
- errors caused by the method and its assumptions.

The first type of error can be calculated using standard error propagation theory. The second type of error is more difficult to assess and requires intercomparison of the methods. All methods use two WVC's in a row, and therefore the orientation or its precision may be a function of WVC number. In the remainder of this chapter the four methods and the error caused by inaccuracies in the WVC positions will be discussed in detail.

2.2 Method 1: Planimetric calculation

The first step in this method is to select two other WVC's on the same row, with coordinates (λ_1, ϕ_1) and (λ_2, ϕ_2). The direction of the line connecting these two points should be perpendicular to the orientation of the WVC under consideration. A good choice seems to locate the two other WVC's symmetrically around the WVC under consideration.

The difference in longitude is $\Delta\lambda = \lambda_2 - \lambda_1$ and that in latitude is $\Delta\phi = \phi_2 - \phi_1$. It is assumed that the second point lies on the right hand side of the first point relative to the satellite moving direction. This means that the WVC number of the second point should be larger than that of the first point.

Assuming that the distance between the two points is short enough to neglect the Earth's curvature, the orientation of a WVC simply equals

$$\alpha = \arctan\left(\frac{\Delta\phi}{\Delta\lambda}\right) \quad . \qquad (2.1)$$

The error in the orientation due to errors in the WVC positions is given by

$$\delta\alpha = \sum_{i=1}^{2} \left| \frac{\partial \alpha}{\partial \Delta\lambda} \frac{\partial \Delta\lambda}{\partial \lambda_i} \right| \delta\lambda + \left| \frac{\partial \alpha}{\partial \Delta\phi} \frac{\partial \Delta\phi}{\partial \phi_i} \right| \delta\phi \quad . \tag{2.2}$$

Evaluating the derivatives yields

$$\delta\alpha = 2\frac{\Delta\lambda\,\delta\lambda + \Delta\phi\,\delta\phi}{(\Delta\lambda)^2 + (\Delta\phi)^2} \quad . \tag{2.3}$$

Note that $\Delta\lambda$ and $\Delta\phi$ are both nonzero, so the error in the orientation obtained this way is regular.

2.3 Method 2: Spherical triangular calculation 1

Assuming the Earth to be a perfect sphere, the "flat Earth" approximation of the previous method can be avoided by using great spherical triangles. Each side of such a triangle is part of a great circle (the intersection of the spherical Earth and a plane passing through the centre of the Earth). For great spherical triangles a sine rule and a cosine rule exist which are the spherical counterparts of the well known sine and cosine rules for triangles in the Euclidian plane. The equator is a great circle, and so are the meridians. Also the satellite orbit projection and the swath are great circles.

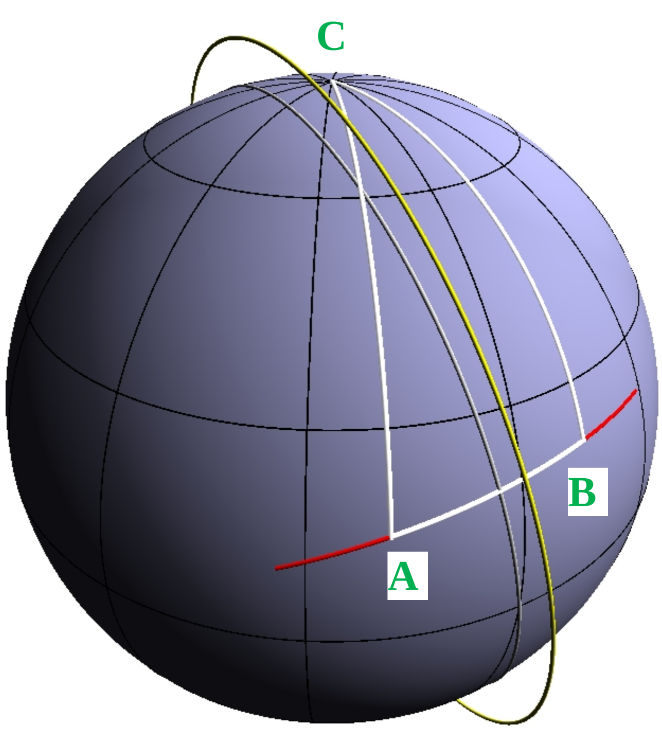

Figure 2.3 Great spherical triangle *ACB* (in white) for method 2. The other colours are the same as in figure 2.1.

Assume now a spherical triangle like in figure 2.3, consisting of the points *A*, *B*, and *C*, with *A* a WVC with coordinates (λ_1, ϕ_1) and orientation α_1, *B* a WVC with coordinates (λ_2, ϕ_2) and orientation α_2, and *C* the North Pole with coordinate $\phi = \pi / 2$. Points *A* and *B* lie on the same row. Triangle *ABC* is a great spherical triangle: side *a* connecting *B* and *C* and side *b* connecting *A* and *C* both lie on a meridian, and side *c* connecting the two WVC's *A* and *B* lies on the satellite swath. Assuming the angles α, β, and γ to be located opposite to sides *a*, *b*, and *c*, respectively, the angle α is the complement of the orientation of WVC *A* and the angle β equals the orientation of WVC *B* plus 90°. The angle γ equals the difference in longitude between *A* and *B*, so $\gamma = \lambda_1 - \lambda_2$. Side *a* equals the difference in latitude between *C* and *A*, $a = \pi / 2 - \phi_2$. In the same way, $b = \pi / 2 - \phi_1$. See also table 2.1.

Point	Coordinates	Side	Arc length	Angle	Value
A	λ_1, ϕ_1	*a*	$\pi / 2 - \phi_2$	α	$\frac{1}{2}\pi - \alpha_1$
B	λ_2, ϕ_2	*b*	$\pi / 2 - \phi_1$	β	$\frac{1}{2}\pi + \alpha_2$
C	$\phi = \pi / 2$	*c*	Eq. (2.6)	γ	$\lambda_1 - \lambda_2$

Table 2.1 Properties of the spherical triangle for finding the WVC orientations.

Application of the sine rule yields

$$\sin\alpha = \sin a \frac{\sin\gamma}{\sin c} = \sin\left(\tfrac{1}{2}\pi - \phi_2\right)\frac{\sin(\lambda_1 - \lambda_2)}{\sin c} \quad , \tag{2.4a}$$

$$\sin\beta = \sin b \frac{\sin\gamma}{\sin c} = \sin\left(\tfrac{1}{2}\pi - \phi_1\right)\frac{\sin(\lambda_1 - \lambda_2)}{\sin c} \quad . \tag{2.4b}$$

The cosine rule for side *c* yields

$$\cos c = \cos\left(\tfrac{1}{2}\pi - \phi_2\right)\cos\left(\tfrac{1}{2}\pi - \phi_1\right) + \sin\left(\tfrac{1}{2}\pi - \phi_2\right)\sin\left(\tfrac{1}{2}\pi - \phi_1\right)\cos(\lambda_1 - \lambda_2) \quad . \tag{2.5}$$

Using table 2.1, this can be simplified to

$$\cos\alpha_1 = \cos\phi_2 \frac{\sin(\lambda_1 - \lambda_2)}{\sin c} \quad , \tag{2.6a}$$

$$\cos\alpha_2 = \cos\phi_1 \frac{\sin(\lambda_1 - \lambda_2)}{\sin c} \quad , \tag{2.6b}$$

$$\cos c = \sin\phi_1 \sin\phi_2 + \cos\phi_1 \cos\phi_2 \cos(\lambda_1 - \lambda_2) \quad . \tag{2.6c}$$

The error in the angle α_i, $i = 1,2$, due to errors in the WVC coordinates equals

$$\delta\alpha_i = \sum_{i=1}^{2} \left|\frac{\partial \alpha_i}{\partial \lambda_i}\right| \delta\lambda + \left|\frac{\partial \alpha_i}{\partial \phi_i}\right| \delta\phi \quad , \tag{2.7}$$

cf. equation (2.2). Some calculus yields for the error in α_1

$$\delta\alpha_1 = \frac{1}{\sqrt{1-X^2}} \left(\left|\frac{\partial X}{\partial \lambda_1}\right| \delta\lambda + \left|\frac{\partial X}{\partial \lambda_2}\right| \delta\lambda + \left|\frac{\partial X}{\partial \phi_1}\right| \delta\phi + \left|\frac{\partial X}{\partial \phi_2}\right| \delta\phi \right) \quad , \tag{2.8a}$$

with

$$X = \frac{\cos\phi_2 \sin(\lambda_1 - \lambda_2)}{\sqrt{1-\cos^2 c}} \quad , \tag{2.8b}$$

and

$$\frac{\partial X}{\partial \lambda_1} = \frac{1}{\sin^2 c} \left(-\sin c \cos\phi_2 \cos(\lambda_1 - \lambda_2) + \frac{\cos c}{\sin c} \cos\phi_2 \sin(\lambda_1 - \lambda_2) \frac{\partial \cos c}{\partial \lambda_1} \right) \quad , \tag{2.8c}$$

$$\frac{\partial \cos c}{\partial \lambda_1} = -\cos\phi_1 \cos\phi_2 \sin(\lambda_1 - \lambda_2) \quad , \tag{2.8d}$$

$$\frac{\partial X}{\partial \lambda_2} = \frac{1}{\sin^2 c} \left(\sin c \cos\phi_2 \cos(\lambda_1 - \lambda_2) + \frac{\cos c}{\sin c} \cos\phi_2 \sin(\lambda_1 - \lambda_2) \frac{\partial \cos c}{\partial \lambda_2} \right) \quad , \tag{2.8e}$$

$$\frac{\partial \cos c}{\partial \lambda_2} = \cos\phi_1 \cos\phi_2 \sin(\lambda_1 - \lambda_2) \quad , \tag{2.8f}$$

$$\frac{\partial X}{\partial \phi_1} = \frac{1}{\sin^2 c} \frac{\cos c}{\sin c} \cos\phi_2 \sin(\lambda_1 - \lambda_2) \frac{\partial \cos c}{\partial \phi_1} \quad , \tag{2.8g}$$

$$\frac{\partial \cos c}{\partial \phi_1} = \cos\phi_1 \sin\phi_2 - \sin\phi_1 \cos\phi_2 \cos(\lambda_1 - \lambda_2) \quad , \tag{2.8h}$$

$$\frac{\partial X}{\partial \phi_2} = \frac{1}{\sin^2 c} \left(-\sin c \sin\phi_2 \sin(\lambda_1 - \lambda_2) + \frac{\cos c}{\sin c} \cos\phi_2 \sin(\lambda_1 - \lambda_2) \frac{\partial \cos c}{\partial \phi_2} \right) \quad , \tag{2.8i}$$

$$\frac{\partial \cos c}{\partial \phi_2} = \sin\phi_1 \cos\phi_2 - \cos\phi_1 \sin\phi_2 \cos(\lambda_1 - \lambda_2) \quad . \tag{2.8j}$$

A similar expression (with $\phi_1 \leftrightarrow \phi_2$) holds for the error in α_2.

2.4 Method 3: Spherical triangular calculation 2

Note that side c of the triangle ABC of the previous section has an arc length of $\Delta s / R$, with Δs the distance between the WVC's A and B, and R the radius of the Earth. Both quantities are known, and using this in the sine rule (2.4) immediately yields

$$\cos\alpha_1 = \cos\phi_2 \frac{\sin(\lambda_1 - \lambda_2)}{\sin\frac{\Delta s}{R}} \quad , \tag{2.9a}$$

$$\cos\alpha_2 = \cos\phi_1 \frac{\sin(\lambda_1 - \lambda_2)}{\sin\frac{\Delta s}{R}} \quad , \tag{2.9b}$$

The error in α_1 due to uncertainties in the WVC positions is given by (2.7), and its reads

$$\delta\alpha_1 = \frac{1}{\sqrt{1 - X^2}} \left(\left|\frac{\partial X}{\partial \lambda_1}\right| \delta\lambda + \left|\frac{\partial X}{\partial \lambda_2}\right| \delta\lambda + \left|\frac{\partial X}{\partial \phi_2}\right| \delta\phi \right) \quad , \tag{2.10a}$$

with

$$X = \cos\phi_2 \frac{\sin(\lambda_1 - \lambda_2)}{\sin\frac{\Delta s}{R}} \quad , \tag{2.10b}$$

and

$$\frac{\partial X}{\partial \lambda_1} = -\cos\phi_2 \frac{\cos(\lambda_1 - \lambda_2)}{\sin\frac{\Delta s}{R}} \quad , \quad \frac{\partial X}{\partial \lambda_2} = \cos\phi_2 \frac{\cos(\lambda_1 - \lambda_2)}{\sin\frac{\Delta s}{R}} \quad , \tag{2.10c}$$

$$\frac{\partial X}{\partial \phi_2} = -\sin\phi_2 \frac{\sin(\lambda_1 - \lambda_2)}{\sin\frac{\Delta s}{R}} \quad . \tag{2.10d}$$

In deriving (2.10c) and (2.10d) it has been assumed that the errors in Δs and R are negligible. A similar expression (with $\phi_1 \leftrightarrow \phi_2$) with holds for $\delta\alpha_2$.

2.5 Method 4: Stereometric calculation

This method is described in [*de Vries and Stoffelen,* 2000], but the derivation will be repeated here for the sake of completeness. Assuming that the Earth is a perfect sphere with radius 1 centred at the origin, the coordinates (λ, ϕ) can be transformed to a three dimensional vector $\mathbf{r}$ according to

$$\mathbf{r} = \begin{pmatrix} x \\ y \\ z \end{pmatrix} = \begin{pmatrix} \cos\lambda\cos\phi \\ \sin\lambda\cos\phi \\ \sin\phi \end{pmatrix} \quad . \tag{2.11}$$

Since $\mathbf{r}$ lies on the surface of the sphere, its length $r = 1$. The unit vectors to the east and the north, $\hat{\mathbf{e}}$ and $\hat{\mathbf{n}}$, respectively, are given as

$$\hat{\mathbf{e}} = \begin{pmatrix} -\sin\lambda \\ \cos\lambda \\ 0 \end{pmatrix} \quad , \quad \hat{\mathbf{n}} = \begin{pmatrix} -\cos\lambda\sin\phi \\ -\sin\lambda\sin\phi \\ \cos\phi \end{pmatrix} \quad . \tag{2.12}$$

Note that these vectors span the tangent plane to the sphere at the point with coordinates (λ, ϕ) .

Now suppose that $\mathbf{r}_1$ and $\mathbf{r}_2$ are the position vectors of two adjacent WVC's on the same row, and that $\mathbf{r}_{12} = \mathbf{r}_2 - \mathbf{r}_1$ is their difference vector. The projection of $\mathbf{r}_{12}$ on the tangent plane spanned by $\hat{\mathbf{e}}$ and $\hat{\mathbf{n}}$ reads

$$\mathbf{p}_{12} = (\mathbf{r}_{12} \cdot \hat{\mathbf{n}})\,\hat{\mathbf{n}} + (\mathbf{r}_{12} \cdot \hat{\mathbf{e}})\,\hat{\mathbf{e}} \quad . \tag{2.13}$$

The orientation α of the WVC at position $\mathbf{r}_2$ is now defined by *de Vries and Stoffelen* [2000] as the angle between $\mathbf{p}_{12}$ and $\hat{\mathbf{e}}$. From the definition of the scalar product and the orthogonality of $\hat{\mathbf{e}}$ and $\hat{\mathbf{n}}$ one readily finds

$$\cos\alpha = \frac{\mathbf{p}_{12} \cdot \hat{\mathbf{e}}}{p_{12}} \quad , \tag{2.14}$$

with $p_{12} = |\mathbf{p}_{12}|$. This definition of the orientation coincides with that of the previous sections. Note that equation (B.9) in *de Vries and Stoffelen* [2000] is not correct.

Substitution of (2.13) into (2.14) and use of the orthogonality of $\hat{\mathbf{e}}$ and $\hat{\mathbf{n}}$ leads to the simple relation

$$\cos\alpha = \frac{\mathbf{r}_{12} \cdot \hat{\mathbf{e}}}{p_{12}} \quad . \tag{2.15}$$

This can be used to simplify the computer code a bit.

It is also possible to derive an expression for the error in α due to errors in the WVC coordinates. This will not be done here, since in the next chapter it will be shown that this method is not to be preferred for calculating the WVC orientation.

3 Results and discussion

The curves in this chapter were made using program `WVCO` (Wind Vector Cell Orientation).

3.1 Comparison

Figure 3.1 shows the four methods as a function of latitude. The curves were obtained using the data in the first three BUFR files of December 1, 2002 processed with SDPv1.2 at 25 km resolution. These three files together contain a bit more than one complete orbit of data. The curves in figure 3.1 pertain to WVC 39, which is only 12.5 km off the satellite ground projection and therefore closely resembles the satellite heading. Comparison with figure 2.1 shows that this is indeed the case. The orientations were calculated for adjacent WVC's (lag size 1).

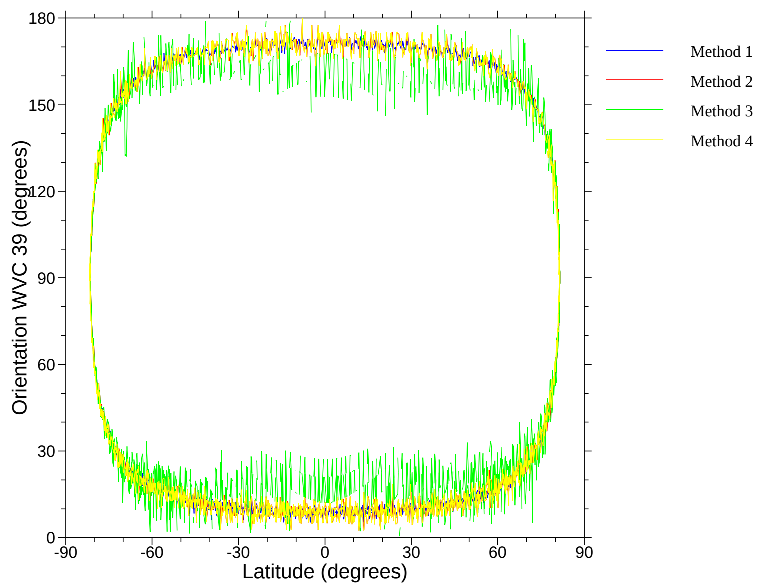

Figure 3.1 The orientation of WVC 39 in the centre of the SeaWinds swath as a function of latitude for the four different methods of calculation.

The most striking feature in figure 3.1 is the noise in the curves. This is due to the fact that all methods used adjacent WVC's with a distance of 25 km. The orientation of the line connecting the two WVC's, and therefore the orientation of both WVC's, is very sensitive to small variations in the position. Therefore errors in the WVC positions have large effect on the orientation.This will be investigated further in the next section.

Figure 3.2 shows the results for method 4. The green curve is produced by the implementation of method 4 in program `WVCO`, the red curve by its implementation in 2DVAR. The 2DVAR implementation contains several bugs. As a result, the diagonalization of the error covariance matrix in the spatial frequency domain is not performed correctly.

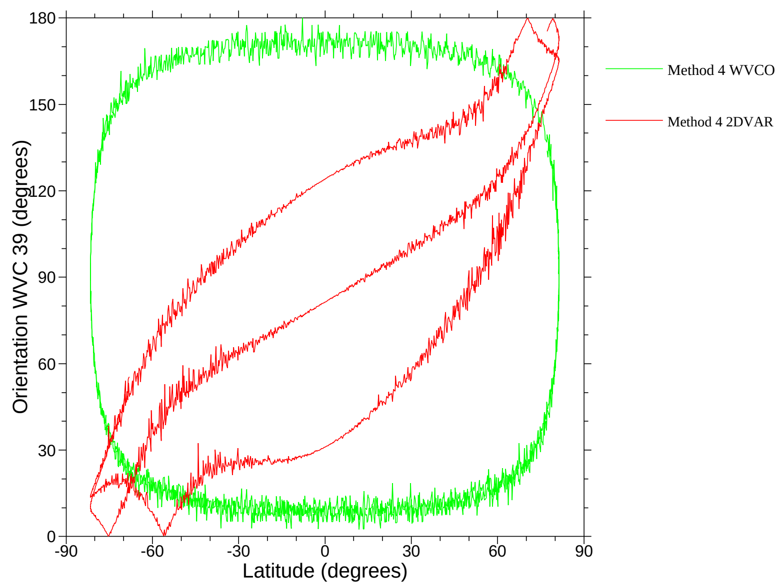

Figure 3.2 The orientation of WVC 38 as a function of latitude for method 4 in the implementation of WVCO (green) and that of 2DVAR (red).

3.2 Lag size

In the previous section it was shown that the orientations for WVC 39 obtained from adjacent WVC's is quite noisy for each method. Figure 3.3 shows in more detail the orientation as function of the latitude, for adjacent WVC's (lag size 1, 25 km, left hand panel) and WVC's with a large separation (lag size 36, 900 km, right hand panel).

Figure 3.4 is similar to figure 3.3, but now the orientation is shown as function of the longitude for only the first two BUFR files of December 1, 2002. The orientations for method 1 were obtained from WVC's located symmetrically around WVC 39. Therefore, the distance between the WVC's for method 1 is actually 50 km (lag size 2) rather than 25 km. The lag size was not set to the maximum possible value of 38 because the coordinates of the first WVC in a row are sometimes missing.

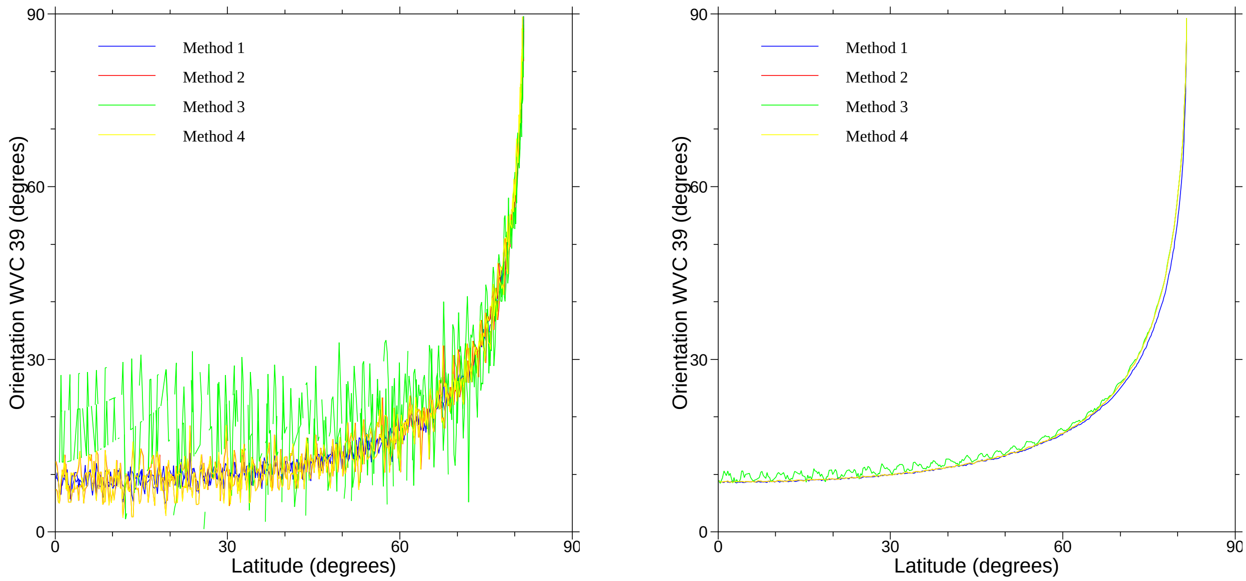

Figure 3.3 Orientation of WVC 39 as a function of latitude for lag 1 (left) and lag 36 (right).

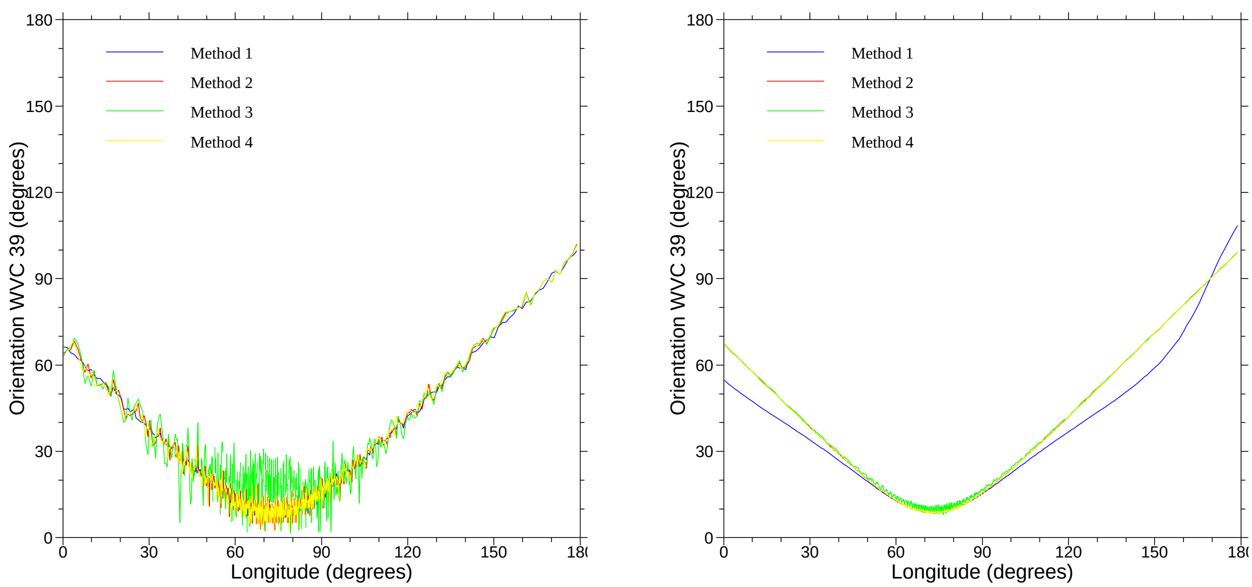

Figure 3.4 Orientation of WVC 39 as a function of longitude for lag 1 (left) and lag 36 (right).

From figures 3.3 and 3.4 it is immediately clear that increasing the lag size (the distance between the WVC's) decreases the error in the orientation caused by uncertainties in the WVC positions. This error appears as noise in the graphs. Note that the curve for method 3 still contains some noise. This is remarkable, since this method is expected to be more precise than method 2 because of its simplicity.

However, method 3 assumes that both the distance between the WVC's and the radius of the Earth contain no error. Due to the fact that the latitude and the longitude of each WVC is given up to 0.01°, the actual distance between the WVC's will not exactly be a multiple of 25 km. This causes an inconsistency in the method which adds noise.

For large lag sizes, method 1 differs from the other methods, as is especially clear from figure 3.4. This deviation is caused by the flat Earth approximation employed in this method. At small lags this approximation is good, but at large lags it introduces a systematic error that is symmetric around an orientation of 90°.

3.3 WVC number

Figure 3.5 shows the orientation of WVC's 3, 39, and 75 as a function of latitude (left hand panel) and longitude (right hand panel) for method 2 with lag size 36. As shown in the previous section, a large lag size is needed to minimize the noise, but then it is not possible to apply method 1 to WVC's 3 and 75, and method 4 to WVC 3. The curves in figure 3.5 were obtained using only the first two BUFR files of December 1, 2002, to avoid overlap. When applicable, methods 3 and 4 give the same results as method 2, though method 3 contains some noise as in figures 3.3 and 3.4 (no results shown). As discussed earlier, this noise is due to deficiencies in the method rather than errors in the WVC coordinates.

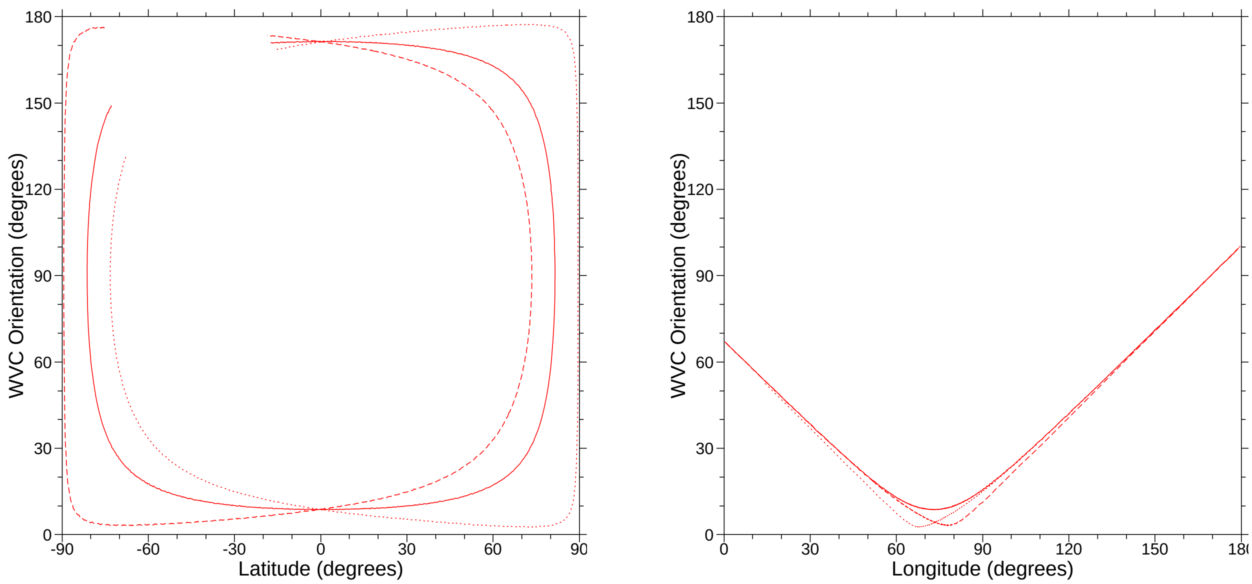

Figure 3.5 The orientation of WVC's 3 (dashed curves), 39 (solid curves), and 75 (dotted curves) as a function of latitude (left) and longitude (right) for method 2.

Note that the orientation of WVC's 3 and 75 is not symmetric around 0° latitude. When QuikSCAT has its largest latitude, WVC 75 is directed towards the North Pole, while WVC 3 is directed away from it. When the satellite has its lowest latitude the situation is reversed: WVC 75 is directed away from the South Pole while WVC 3 is directed towards it. This causes the asymmetry in the left hand panel of figure 3.5. Also the position where the orientation is minimal (or maximal) varies with WVC number.

Note that the coordinates in figure 3.5 are the coordinates of the WVC under consideration. Therefore figure 3.5 gives no information on the variation in orientation along a single row, because each WVC has different coordinates. Figure 3.6 shows the range in the orientation as a function of the satellite position. The range in the orientation is defined as the absolute difference between the orientations of WVC 3 and of WVC 75 (distance 1800 km). The position of the QuikSCAT satellite is set equal to the average of the positions of WVC 38 and 39. The left hand panel of figure 3.6 was obtained from the first three BUFR files of December 1, 2002; the right hand panel from only the second BUFR file.

Figure 3.6 shows that the range in WVC orientation is small along the equator (latitude equal to 0°, longitudes around -120° and +70°) and increases towards the poles to a maximum value of more than 70°. At the points of minimum and maximum latitude the orientation is 90° for all WVC's, so the range in WVC orientation quickly passes 0° here.

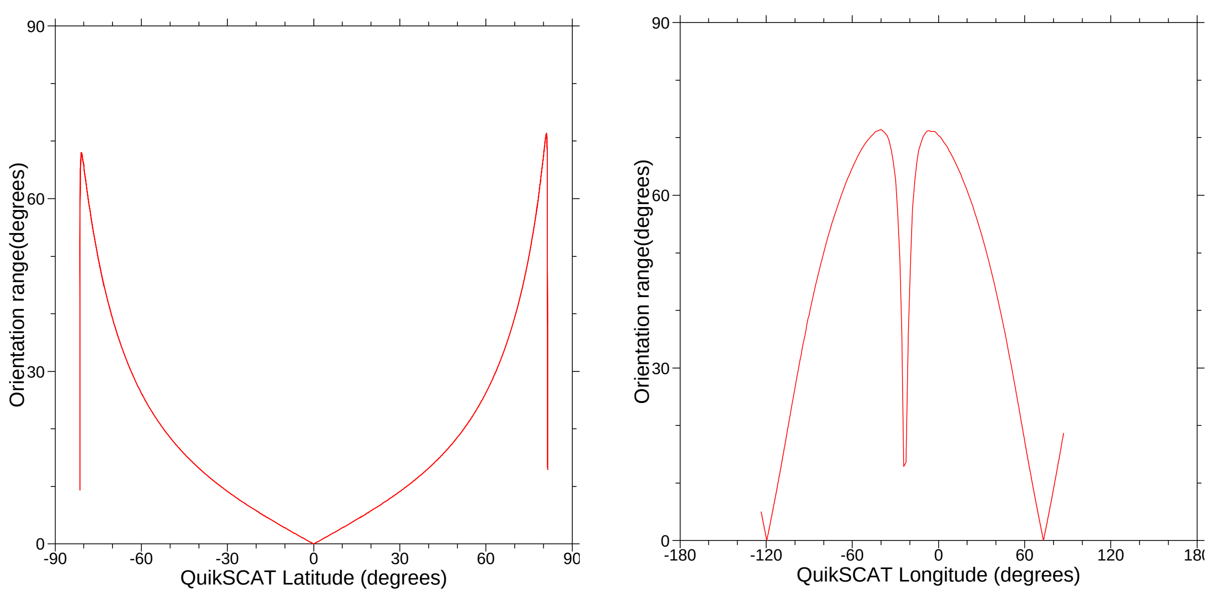

Figure 3.6 The range in orientation for method 2 as a function of the satellite latitude (left) and longitude (right).

3.4 Effect of errors in WVC position

Figure 3.7 shows the error in the orientation of WVC 39 caused by errors in the WVC coordinates as a function of longitude for methods 1 (blue curve), method 2 (red curve), and method 3 (green curve), all with a lag size of 36. The curves were obtained from the second BUFR file of December 1, 2002, and the expressions from chapter 2.

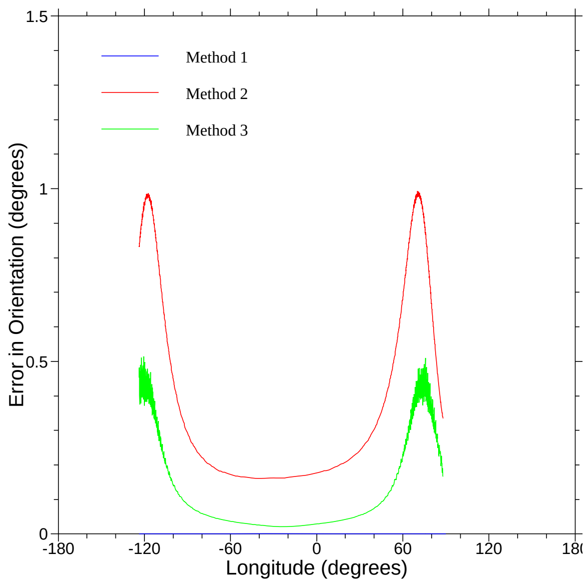

Figure 3.7 The error in the orientation as a function of longitude for methods 1 (blue), 2 (red), and 3 (green).

Note that this error is smallest for method 1: the curve coincides with the x-axis on the scale of figure3.7. For method 3 the error is about half of that of method 2, while the results presented before indicate that method 3 is the noisiest of all methods. This is because the error for method 3 was derived from the assumption that the error in the distance between the WVC's is negligible compared to the positions of both WVC's. However, this distance depends on the positions and should be taken into account.

The error in method 2 is about 1° at most. The largest error is found near the equator.

3.5 Discussion

In the previous sections four methods for calculating the orientation of a WVC were investigated in more detail. All methods need at least one additional WVC for the calculation of the orientation. Each method therefore is a function of the lag, the distance between the WVC's.

All methods are noisy for lag size 1. This noise is due to the propagation of errors in the WVC coordinates to the orientations. To minimize it, the lag must be chosen as large as possible. This rules out method 1, planimetric calculation, because the flat Earth approximation employed here is no longer valid for large lag sizes. Moreover, this implies that the methods that were implemented in ASAC and 2DVAR up to 2006 need to be upgraded – which in the meantime has been done.

The method must be applicable for all WVC's in a row. Method 4 assumes that the orientation of a WVC can be found from that WVC and one left of it, with smaller WVC number. This is not possible for the WVC's at the start of each row, so this rules out method 4. In theory, the error in the orientation due to uncertainties in the WVC coordinates are smaller for method 3 than for method 2, but under the false assumption that the distance between two WVC's is free of errors. This deficiency in method 3 adds noise, and method 3 turns out to be the noisiest of all methods.

Therefore method 2 remains. It seems relatively free of errors caused by deficiencies in the method, though it assumes the Earth to be a perfect sphere. The error in the orientation caused by errors in the WVC positions is 1° at most.. Note, however, that the derivation of method 4 in section 2.5 could be done with the role of the two WVC's reversed. This possibility will not be pursued further here, as method 4 is computationally less efficient than method 2, and no improvement is expected in the error due to uncertainties in the WVC coordinates..

A very efficient algorithm to calculate the orientation of all WVC's in a row of SeaWinds data at 25 km resolution would be to calculate the orientations of WVC 1 and WVC 39, WVC 2 and WVC 40, etc, until WVC 38 and WVC 76. Each step yields two orientations, and the lag size is 38 (distance 950 km) for each WVC, so the lag dependent error in the orientation is the same along each row.
Another possibility, the one actually implemented in 2DVAR, is to find the maximum lag for each pair to minimize the error. This approach is more general when data are missing, like at the beginning and end of each BUFR file. See also chapter 5.

4 Heading

4.1 Methods

Once the orientation of each WVC can be calculated, the heading of the satellite can be obtained. In general the coordinates of the ground projection of the satellite don't coincide with the coordinates of a WVC. Only at 100 km resolution the centre of WVC 10 coincides with the satellite projection. In the other cases the position of the ground projection of the satellite can be obtained by averaging the positions of WVC's on either side of the ground track, as already has been done in chapter 3 to obtain the QuikSCAT position for figure 3.6.

As argued in the last section of chapter 3, method 2 is suited well to calculate the WVC orientation, and hence the satellite heading. There exists, however, another simple formula for the satellite heading that can be derived using great spherical triangles.

4.2 Spherical trigoniometric method

There is simple expression for the satellite heading that can be obtained from a great triangle formed by the points $A(\lambda,\phi)$, the position of the satellite, $M(\lambda_M,\phi_M)$, the point where the satellite has its highest latitude, and C, the North Pole. Note that the satellite crosses the local meridian at right angles when it is in it largest or smallest latitude.

Point	Coordinates	Side	Arc length	Angle	Value
A_0	$\lambda_0, 0$	a	Eq. (4.1)	α_0	8.62°
C	$\phi = \pi/2$	c		γ	
M	λ_M, ϕ_M	m	$\pi/2$	μ	$\pi/2$

Table 4.1 Properties of the spherical triangle for finding the maximum latitude of the satellite orbit.

To obtain the latitude of point M, first suppose that $A = A_0$ lies on the equator. The angle α_0 then equals the inclination of the QuikSCAT orbit, $\iota = 8.62^\circ$ [*Freilich*]. The properties of triangle A_0CM are listed in table 4.1, and the triangle is shown in figure 4.1. The sine rule immediately gives

$$\frac{\sin a}{\sin \alpha_0} = \frac{\sin m}{\sin \mu} = 1 \quad , \tag{4.1}$$

so $a = \alpha_0$ and the maximum latitude of the satellite orbit ground projection is $\phi_M = \pi / 2 - \alpha_0$, which equals 81.38°.

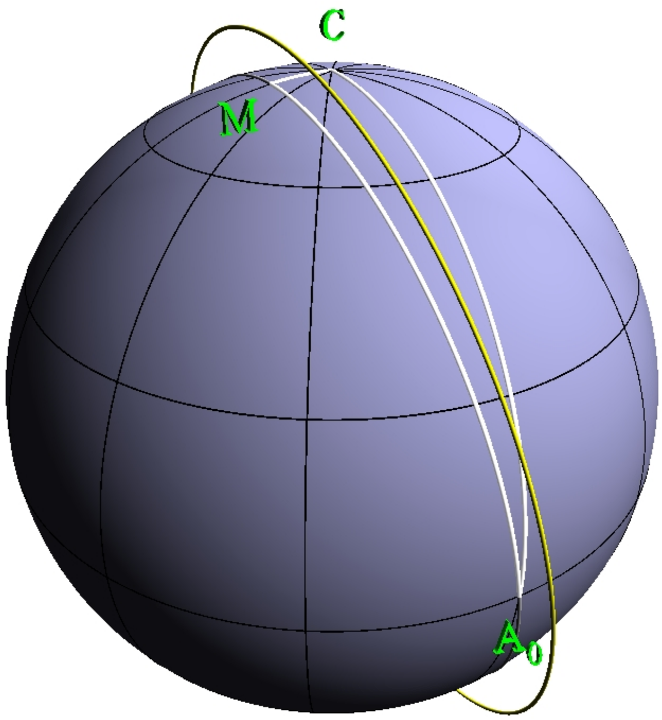

Figure 4.1 Great spherical triangle A_0CM to find the coordinates of point M.

Next, suppose that point A lies somewhere on the ground projection of an ascending orbit, like in figure 4.2, so that A lies east of M and consider the great triangle ACM. Its properties are given in table 4.2.

Point	Coordinates	Side	Arc length	Angle	Value
A	λ, ϕ	a	$\alpha_0 = 8.62^\circ$	α	Eq. (4.3)
C	$\phi = \pi / 2$	c		γ	
M	λ_M, ϕ_M	m	$\pi / 2 - \phi$	μ	$\pi / 2$

Table 4.2 Properties of the spherical triangle for finding the heading of the satellite.

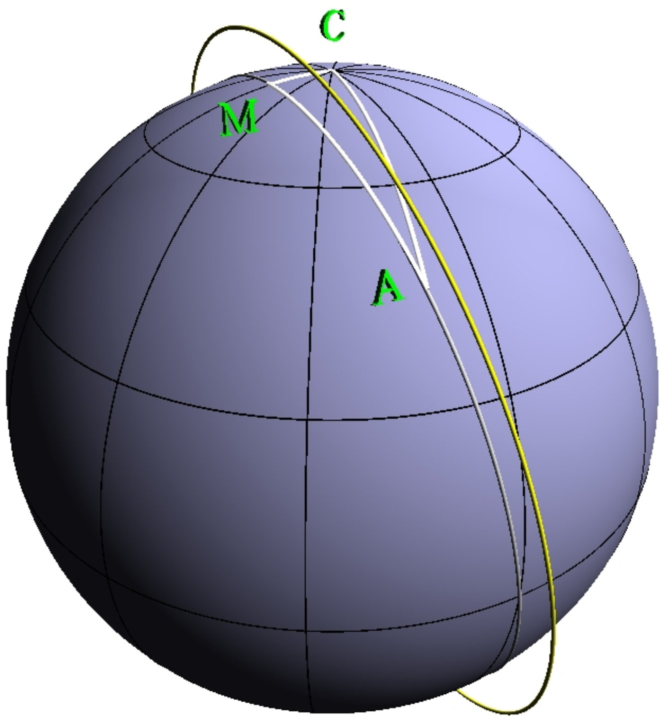

Figure 4.2 Great spherical triangle ACM for finding the satellite heading.

The sine rule yields

$$\frac{\sin a}{\sin \alpha} = \frac{\sin m}{\sin \mu} \Leftrightarrow \sin \alpha = \frac{\sin \alpha_0 \sin \frac{1}{2}\pi}{\sin(\frac{1}{2}\pi - \phi)} \quad . \tag{4.2}$$

Therefore the satellite heading α satisfies

$$\alpha = \arcsin\left(\frac{\sin \alpha_0}{\cos \phi}\right) \quad , \quad \text{ascending orbit.} \tag{4.3a}$$

The heading is a function of the latitude and the inclination only, as may be expected. Note that at the highest point of the satellite orbit $\phi = \phi_M = \frac{1}{2}\pi - \alpha_0$, and $\alpha = \arcsin(1) = 90^\circ$, in agreement with the definition of α being measured counterclockwise from the north.

For the descending part of the orbit, where A lies west of M, the derivation is the same as for the ascending part, but with the angle α replaced by $\alpha - \pi$. This gives

$$\alpha = \pi - \arcsin\left(\frac{\sin\alpha_0}{\cos\phi}\right) \quad , \quad \text{descending orbit.} \tag{4.3b}$$

When $\phi = \phi_M$, equation (4.3b) yields $\alpha = 90^\circ$ as before. When $\phi = 0$ (descending node), equation (4.3b) yields $\alpha = 180^\circ - 8.62^\circ = 171.38^\circ$.

The error in α due to errors in the satellite position and its inclination equals

$$\delta\alpha = \left|\frac{\partial\alpha}{\partial\phi}\right|\delta\phi + \left|\frac{\partial\alpha}{\partial\alpha_0}\right|\delta\alpha_0 \quad , \tag{4.4}$$

where $\delta\alpha_0 = 0.005^\circ$ is the error in the inclination. From (4.3a) and (4.3b) one readily finds

$$\delta\alpha = \frac{\left|\frac{\sin\phi}{\cos\phi}\sin\alpha_0\right|\delta\phi + \left|\cos\alpha_0\right|\delta\alpha_0}{\sqrt{\cos^2\phi - \sin^2\alpha_0}} \quad . \tag{4.5}$$

Equation (4.5) shows that the error in α diverges like $x^{-1/2}$ for any finite value of $\delta\phi$ and/or $\delta\alpha_0$ when $\cos\phi = \pm\sin\alpha_0$. The situation $\cos\phi = \sin\alpha_0$ occurs when the ground projection of the satellite orbit reaches its highest or lowest latitude. The derivative of the inverse sine goes to infinity, so in these regions (4.3a) and (4.3b) are less suitable for calculating the satellite heading. Use of the series expansion of $\arcsin(1-y)$ [*Abramowitz and Stegun*, 1970, 4.4.41] makes no difference, since it has the same divergent behavior.

The expressions presented in this section can also be obtained using a great spherical triangle AA_0C, with the ascending node instead of the point with maximum latitude. However, the different behavior of the ascending and descending part of the orbit is less obvious then.

4.3 Results

Figure 4.1 shows the heading of QuikSCAT as a function of latitude for method 2 of chapter 2 (red curve) and the alternative method of section 4.2 (blue curve). The methods show little difference, though method 2 seems to contain more noise when the satellite is near its minimum or maximum latitude.

Figure 4.2 shows the error in the orientation caused by errors in the satellite position, WVC positions and/or inclination, as a function of longitude for both methods. The curves were obtained from the second BUFR file of December 1, 2002. The divergence in the error of the alternative method when the satellite is at its minimum or maximum latitude is clearly visible. Moreover, due to the flattening of the Earth at the poles, the latitude of the satellite can become larger in absolute value than expected for a perfect sphere. As a result, the argument of the inverse sine in (4.3) can become larger than 1, so the heading does not exist in these cases.

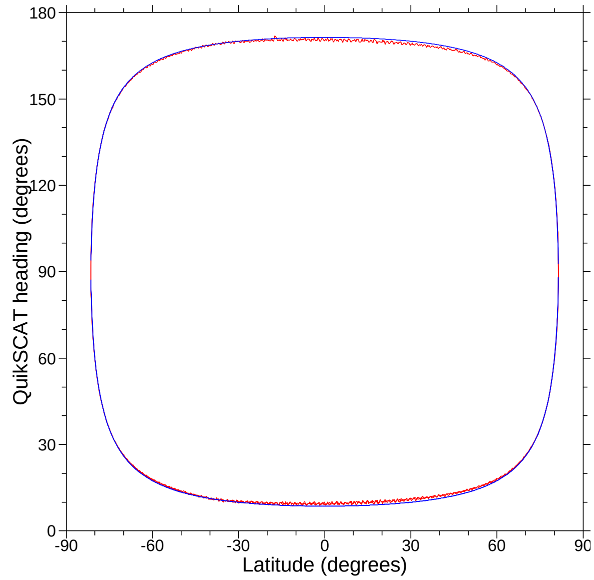

Figure 4.1 QuikSCAT heading as a function of latitude for method 2 (red) and the alternative method presented in section 4.2 (blue).

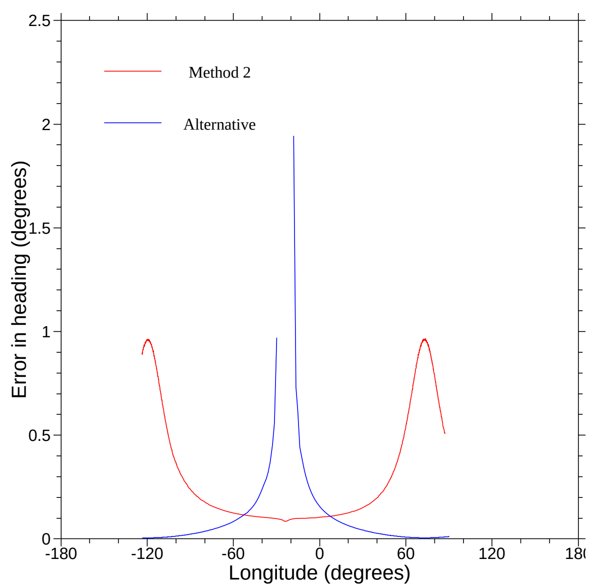

Figure 4.2 Error in heading as a function of longitude for method 2 (red) and the alternative method (blue).

Figures 4.1 and 4.2 show that the methods are each others complement as far as the error in the heading due to uncertainties in satellite position, WVC coordinates, and inclination is concerned: for the alternative method this error diverges when the satellite is near its minimum or maximum latitude, but there method 2 exhibits the smallest error. Near the equator, where method 2 shows the largest error, the error for the alternative method is smallest. The optimal method for finding the heading of the satellite will therefore be a combination of both methods, and has an error of less than.0.2°.

5 Effects on 2DVAR

5.1 Routine `Set_WVC_Orientations`

The orientation of the WVC's is needed in 2DVAR module `Ambrem2DVAR` in directory `genscat/ambrem` [*SCAT group*, 2006]. In the old versions (up to CVS version 1.20), the WVC orientations were calculated by subroutine `SetAlpha`. From version 1.21 onwards, this is done by routine `Set_WVC_Orientations`. This routine needs subroutine `WVC_Orientation` in module `convert.F90` from `genscat/support/convert`.

Routine `Set_WVC_Orientations` calculates the WVC orientations from WVC's with as large as possible separation. This approach is not the most efficient in terms of computation time, but it minimizes the errors in the heading. Since there is no lower limit on the separation (as long as it is nonzero), it yields orientations for every row that contains at least two WVC's from which the position is given, so it can cope with the semicircle of missing data at the start and end of each SDP BUFR file.

`Set_WVC_Orientations` also contains a post processing step. If a WVC contains no positions, but its direct neighbours do, the orientation in that WVC is set equal to the average of its neighbours' orientations. If the first WVC of a row contains no position, but the second and third do, the orientation of the first WVC is found from linear extrapolation as

$$\alpha_1 = 2\alpha_2 - \alpha_3 \quad , \tag{5.1}$$

where α_i stands for the orientation of WVC number i.Similarly, the last WVC of a row is calculated from its two neighbours as

$$\alpha_N = 2\alpha_{N-1} - \alpha_{N-2} \quad , \tag{5.2}$$

with N the number of WVC's in a row.

5.2 Results

Figures 5.1 and 5.2 show two wind fields on the southern hemisphere for January 1, 2001 obtained with SDP without MSS (Test 1, see *SCAT Group* [2006]). Figure 5.1 was obtained with the old routine `SetAlpha`; figure 5.2 with the new routine `Set_WVC_Orientations`.

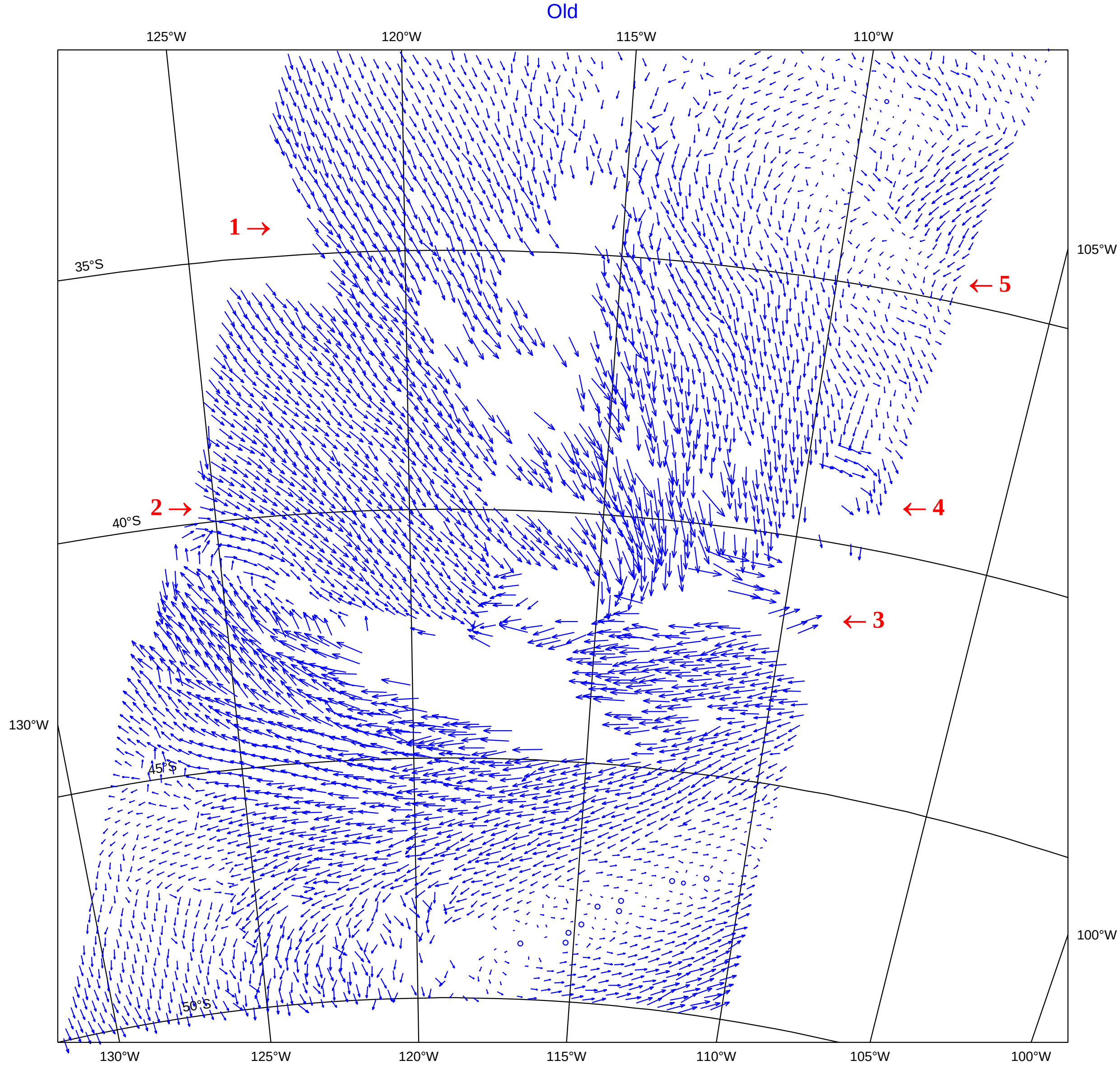

Figure 5.1 Wind field for January 1, 2002 obtained from SDP without MSS using the old routine `SetAlpha`.

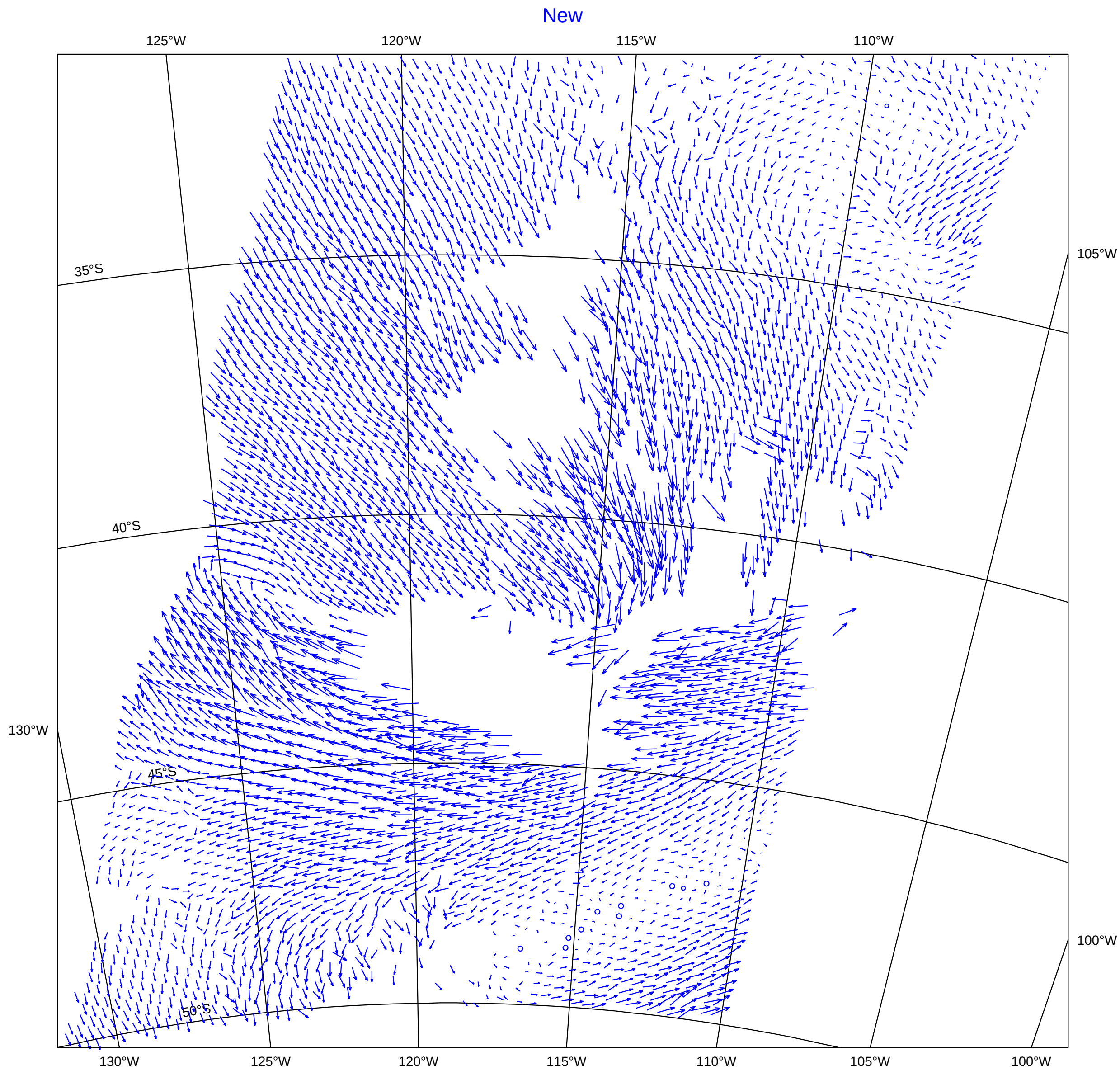

Figure 5.2 As figure 5.1, but for the new routine Set_WVC_Orientations.

The difference between the two wind fields was analyzed using program BAT. The results of this analysis is given in table 5.1. The table shows that there are over 1500 differences. In more than 700 cases there is a diference in the WVC Quality Flag, mostly in bit 10 (KNMI+JPL Quality Flag), but 25 times in bit 5 (σ_0 too large). In the remaining cases the difference is in the index of the selected solution.

BUFR item	Parameter	Number of differences
21, bit 10	WVC Quality Flag, KNMI+JPL QC flag	699
21, bit5	WVC Quality Flag, σ_0 too large	20
25	Selection index	818
	Total	**1537**

Table 5.1 Differences in SDP testrun.

Note that figures 5.1 and 5.2 contain only a part of the complete BUFR file. Yet, some of the differences from table 5.1 are visible. They are indicated by the numbered red arrows in figure 5.1. At 1, there are wind vectors missing in figure 5.1 that are present in figure 5.2. At 2, 3, and 4 the situation is reversed: wind vectors present in figure 5.1 are absent in figure 5.2. This is caused by differences in the WVC Quality Flag: if bit 10 of this flag is set, the corresponding wind vector is not plotted in figure 5.1 or 5.2. At 5, but also at 4, some changes in wind direction can be seen. These are manifestations of a different choice in the selection index.

It is not possible to say which of the figures 5.1 and 5.2 shows the best wind field. Either of the figures has its strengths and weaknesses. Further investigation to the implementation of 2DVAR and the value of the parameters controlling it is necessary.

6 Other platforms

The WVC orientation can best be calculated c using the sine and cosine rules on a great spherical triangle formed by two WVC's on a single row (points *A* and *B*) and the North Pole (point *C*). The equations read (see section 2.3)

$$\cos\alpha_1 = \cos\phi_2 \frac{\sin(\lambda_1 - \lambda_2)}{\sin c} \quad , \tag{6.1}$$

$$\cos\alpha_2 = \cos\phi_1 \frac{\sin(\lambda_1 - \lambda_2)}{\sin c} \quad , \tag{6.2}$$

$$\cos c = \sin\phi_1 \sin\phi_2 + \cos\phi_1 \cos\phi_2 \cos(\lambda_1 - \lambda_2) \quad . \tag{6.3}$$

where point *B* is to the right of point *A*, i.e., the WVC index of point *B* is higher than that of point *A*, assuming that the WVC's are counted from left to right with respect to the platform direction. Note that angles α and β are measured counterclockwise, α from line *c* to line *b*, and β from line *a* to line *c*.

Note that (6.3) does not depend on the sign of $\lambda_1 - \lambda_2$. For ascending passes *A* lies westward of *B*, so we have $\lambda_1 > \lambda_2$, and both α_1 and α_2 have a value between 0° and 90°. For descending passes, *A* lies eastward of *B*, so we have $\lambda_1 < \lambda_2$, and the cosines in (6.1) and (6.2) change sign. As a result, both α_1 and α_2 have a value between 90° and 180°, and (6.1) – (6.3) give the correct answer.

Equations (6.1) – (6.3) can be derived for descensing passes in the same manner as done in section 2.3. One must keep in mind that for descending passes the orientation of the great spherical triangle *ABC* changes sign. Angle γ changes sign because λ_1 and λ_2 interchange, as already stated above, while angles α and β are now measured clockwise.

This procedure, encoded in routine `WVC_Orientation`, can be applied to all polar orbiting satellites. These are moving from east to west, and always have $\phi_1 > \phi_2$, or, in other words, the WVC with the lower index has a smaller latitude than the WVC with the higher index.

For RapidSCAT on board the International Space Station (ISS) the situation is different: this platform moves from west to east, opposite to the polar orbiting satellites. If the WVC index of point *B* is larger than that of point *A* (point *B* to the right of point *A* on the swath), application of (6.1) – (6.3) will yield descending results (α_1 and α_2 between 90° and 180°) for ascending passes and ascending results (α_1 and α_2 between 0° and 90°) for descending passes.

If we denote the outcome of `WVC_Orientation` with points A and B interchanged by α_1^{rev} and α_2^{rev}, then we have

$$\alpha_i^{rev} = \pi - \alpha_i \quad , \quad i = 1,2 \quad . \tag{6.4}$$

Moreover, the RapidSCAT WVC orientations are 180° larger than the polar satellite WVC orientations, so

$$\alpha_i^{RapidSCAT} = \pi + \alpha_i \quad , \quad i = 1,2 \quad . \tag{6.5}$$

Combining (6.4) and (6.5) yields

$$\alpha_i^{RapidSCAT} = 2\pi - \alpha_i^{rev} \quad , \quad i = 1,2 \quad . \tag{6.6}$$

So the RapidSCAT WVC orientation is obtained by calling `WVC_Orientation` in the usual way and subtracting its outcome from 360°. One can distinguish the two platform types by the latitude of two WVC's in a row: for RapidSCAT the WVC with the lower index has the higher latitude throughout the orbit while for the polar satellites the WVC with the lower index has the lower latitude.

7 Conclusions

The methods for calculating the WVC orientation currently employed in program ASAC and in 2DVAR are not precise enough and need upgrading.

A suitable method for calculating the orientation of a WVC is using the sine and cosine rules on a great spherical triangle formed by two WVC's on a single row and the North Pole. The separation of the two WVC's should be as large as possible. This method is described as method 2 in chapter 2. A suitable algorithm for finding the orientations of all WVC's on a row was given at the end of chapter 3. The error in the orientations due to errors in the WVC positions is 1° at most. Additional errors may arise because the Earth is assumed to be a perfect sphere, but these errors are systematic in nature and are expected to be small.

A modification of method 4 could be an alternative. However, it is not expected to be more precise than the method outlined above, considering the effect of errors in the WVC positions as well as systematic effects. Moreover, it is computationally less efficient.

Averaging the orientations of the central WVC's yields a good estimate for the heading of the satellite near the poles. Near the equator, an alternative spherical trigoniometric method presented in chapter 4 is more accurate. When combining both methods in an optimal way, the error in the heading caused by errors in satellite position, WVC coordinates, and inclination of the satellite orbit is less than 0.2°.

The method chosen for calculating the WVC orientation has a clear impact on the wind fields produced by 2DVAR. However, more detailed investigations are needed to state if a better calculation of the WVC orientations leads to improved wind fields.

References

Abramowitz, M.A., and Stegun, I.R., 1970,
Handbook of Mathematical Functions.
Dover Publications, New York, USA.

Freilich, M.H.,
SeaWinds Algorithm Theoretical Basis Document.

SCAT Group, 2006,
(de Kloe, J., Portabella, M., Stoffelen, A., Verhoef, A., Verspeek, J., and Vogelzang, J.)
SDP user manual and reference guide, version 1.3.
NWP SAF document NWPSAF-KN-UD-002, KNMI, de Bilt, The Netherlands.

de Vries, J., and Stoffelen, A., 2000,
2D Variational Ambiguity Removal.
Internal Report, KNMI.